Usage of global navigation systems for detection of dangerous meteorological phenomena

V F Kravchenko[1], O V Kravchenko[1], V I Lutsenko[2], I V Lutsenko[2], D O Popov[2]

(1. *Kotel'nikov Institute of Radio Engineering and Electronics, Russian Academy of Sciences, Moscow 125009, Russia;*

2. *Usikov Institute of Radiophysics and Electronics, National Academy of Sciences of Ukraine, Kharkov 61085, Ukraine*)

Abstract: The method of dangerous meteorological phenomenon detection using the data of coordinate measurement by receivers of global navigation satellite system (GLONASS) and global positioning system (GPS) is proposed. The possibility of thunderstorm courses and strong clouds detection on data of pseudo-distances and altitudes is shown theoretically and confirmed experimentally.

Key words: dangerous meteorological phenomenon; radio-raying; global navigation system; pseudo-range; altitude

0 Introduction

Many atmospheric phenomena are dangerous for aviation and sea transport. And some meteorological values have to be measured very precisely for modern aircraft and ships safety. Therefore, for the needs of the aviation and fleet, it is necessary to introduce the means and methods for calculation of the future state of the meteorological variables (air pressure, wind and air temperature) calculation of movement and evolution of the dangerous synoptic objects such as cyclones, theirs hollows with atmospheric fronts, anti-cyclones crests, etc. Synoptic processes (atmospheric fronts, heavy convective instability and extremely powerful progress of cumulonimbus cloudiness) lead to appearance of some dangerous meteorological phenomena. At presence of some of the phenomena there are bulk of humidity, ice and sand in the atmosphere. Therefore, the development of new methods for detection dangerous meteorological phenomena using radiation of Earth, artificial satellites and navigation satellites specifically is in great interest[1]. Difference of dielectric properties for that atmosphere parts in which are the dangerous phenomena like cumulonimbus clouds are moisture-laden from standard, can be the background for the dangerous phenomena detection.

1 Results of dangerous meteorological phenomena detection

Navigation problem of detection of the object positioning is solved by measuring distance minimum up to three satellites (pseudo-ranges up to four satellites). At that the object position defines the three radius vectors $\boldsymbol{R}_i$, the position of which in the polar coordinates defines by azimuth φ_i and elevation observation angles β_i of i-satellite. Troposphere refraction and troposphere heterogeneity presence, for example, as moisture-laden clouds lead to increasing of pseudo-distances to navigation satellite and appearance of errors of positioning measurement $\delta\boldsymbol{R}_i$ relatively to each of satellite and sum error of coordinate's estimation is described by radius vector $\boldsymbol{\delta} = \sum_{i=1}^{3}\delta\boldsymbol{R}_i'$. Electric way lengthening of electromagnetic wave propagation is defined at dielectric capaci-

tivity of the environment which, first of all, will be defined by a moisture stock. Dependencies of the real n' and imaginary n'' parts of freshwater refraction coefficient on temperature obtained using results[2] are in Table 1.

Table 1   Dielectric parameters of freshwater for frequency 1 590 MHz

t (℃)	n'	n''
0	9.26	0.81
10	9.10	0.58
20	8.91	0.42
30	8.76	0.31
40	8.53	0.23

These data are calculated for mean frequency 1 590 MHz of operating band of GPS (1 575 MHz) and GLONASS (1 602 MHz) systems.

Ice real and imaginary parts of refraction coefficient practically do not depend on wave length (in the centimeter band). Refractive index therewith does not depend on temperature and equals 1.78. The data[3] about temperature dependence n'' are presented in Table 2.

Table 2   Ice dielectric parameters[3]

t (℃)	n'	n'' (10^4)
0	1.78	24
−10	1.78	7.9
−20	1.78	5.5

Specific attenuation of ice is determined by the equation[4] $\gamma = \dfrac{3\pi}{\lambda\rho}a_1 W$, where λ is wavelength, ρ is density, a_1 is a constant, W is water content. Spatial characteristics for different types of meteorological formations and their water content are presented in Table 3. Rain parameters imported from Ref. [5] are

shown in Table 4.

Table 3   Water content and spatial characteristics of meteorological formations[5]

Type of formation	Size (km)		Water content (g/m³)	
	ΔX	ΔY	$\overline{W}$	max$W$
Fog	100—1 000	0.3—2.3	0.25	0.88
Layered clouds	1 000	1—4	0.1	0.4
Cumulus clouds	10	10	0.4	1.7
Cumulonimbus clouds	15—20	2—10		

Table 4   Parameters of rains

Type of rain	d (mm)	W (g/m³)	I (mm/h)
Small	0.20	0.093	0.25
Light	0.45	0.140	1.00
Moderate	1.00	0.280	4.00
Strong	1.50	0.830	15.00
Very strong	2.10	1.800	40.00
Downpour	3.50	5.400	100.00

The dependence of the water content of the precipitation against their intensity in logarithmic scale[5], as well as linear and parabolic approximation of this dependence is shown in Fig. 1.
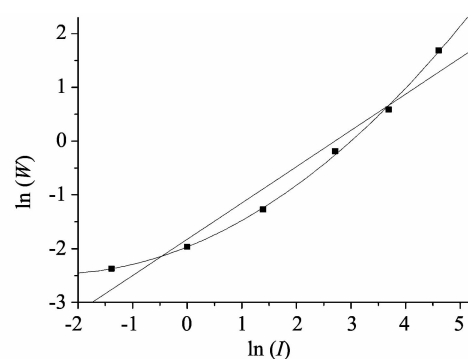

Fig. 1   Dependence of water content of heavy rainfall upon intensity

It can be seen that the best results are obtained by the parabolic approximation

$$\ln(W) = A + B_1\ln(I) + B_2(\ln(I))^2. \quad (1a)$$

The values of coefficients are given in Table 5.

Table 5   Approximation of water content and intensity of rain

	Type of approximation	A	B_1	B_2	R	SD	N	P
Water content of average intensity	Linear	−1.835	0.675	—	0.979	0.361	6	6.82×10^{-4}
	Quadratic	1.97	0.408	0.083	0.999	0.063	6	<0.000 1
Average intensity of the maximum	Quadratic	−0.234	−0.23	5×10^{-4}	0.66	18.9	9	0.041

In Table 5, R is the coefficient of correlational, SD is the RMS error the approximation and N is the number of measurement points.

The correlation coefficient of data is more than 0.99. Empirical expression for the dependence of the water content against precipitation intensity has the form

$$\ln(W) = -1.97 + 0.408\ln(I) + 0.083(\ln(I))^2. \quad (1b)$$

Spatial correlation function of heavy rain[5] described by the expression $\rho(l) = \exp(-0.2l)$. It takes into account the fact that the correlation l_0, where the value $\rho(l)$ decreases in e-times relative to the maximum, is approximately 5 km[6]. Maximum amount of precipitation I_{max} is approximately in 2 times greater than their average intensity.

To account for the influence of meteorological formations on the phase delay and attenuation of the signal, the cloud cover model can be used[7]. In this case, introduced by meteorological formations in the signal per unit length, the damping γ and elongation of electrical path length δr depend on the water content of precipitation W and the values of the real part of the refractive index n'

$$\gamma = 10\lg e \times 10^{-3}Wn'',$$

$$\delta r = 10^{-3}W(n'-1). \quad (2)$$

The elongation of the electrical length path leads to an additional phase shift propagating through the zone of precipitation waves. Thus, the presence of moisture or dust particles in meteorological hazards affect both the amplitude and the phase delay of the signal received from the satellite. This influence can be detected by measuring the change in the satellite's pseudo-range, coordinates and altitude of the measuring points, as well as the interference pattern of the received field. The change of pseudo-range Δr by passing an electromagnetic wave through a zone with increased moisture reserves W and length Δl_0 will be $\Delta r = \delta r \Delta l_0$, wherein at small angles the length of the zone will be approximately correspond to its horizontal extent, for heavy rains which constitute about 5 km. Expression for Estimation of maximal increments of pseudo-range max δr to the satellite due to the presence in the propagation path of precipitation

with regard to Eq. (2) has the form

$$\max \delta r [\text{m}] = 10^{-3} l_0 W_{max} [\text{g/m}^3](n'-1), \quad (3)$$

where $l_0 = \begin{cases} h_y/\sin\beta \leqslant h_x \\ h_x \end{cases}$ is path length of radio waves in precipitation; h_x and h_y are lengths of cloudiness in the horizontal and vertical planes, respectively; β is the elevation angle of the satellite.

Using data of the refractive indices (Tables 1 and 2), the relation is established between the water content and the intensity of precipitation (1), as well as the dependence of the Maximum amount of precipitation against their average intensity. The expected increment of pseudo-ranges upon the intensity of rainfall and elevation of the satellite are estimated as Fig. 2.
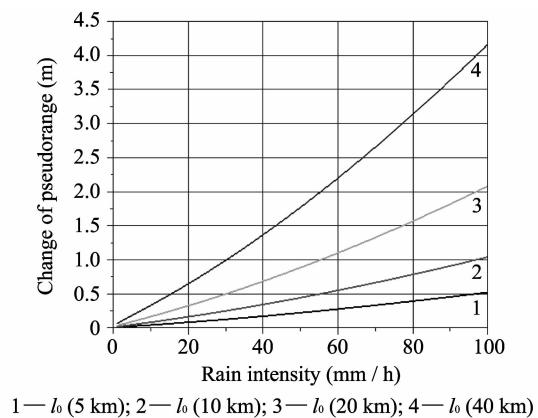

1 — l_0 (5 km); 2 — l_0 (10 km); 3 — l_0 (20 km); 4 — l_0 (40 km)

Fig. 2　Dependence of pseudo-range increment against intensity of rainfall and the sizes of their area

It is seen that heavy rains may lead to changes of pseudo-ranges, which can reach several meters. In experimental studies, the antenna of measuring receiver was located at a height of 30 m above the Earth's surface. For the experimental investigations, the receiver CH-4701 and CH-4706 of the signals GPS, GLONASS, GNNS are used. It is developed and manufactured by construction department "NAVIS", Smela, Mazura st. 24, Ukraine, 20708.

Since the sensitivity to the presence of clouds increases at low elevation angles, and the length of the path in the sediments increases, the measured of pseudo-range to the satellite was at radio occultation. Fig. 3 shows the variation of root-mean-square (RMS) fluctuations of pseudo-range to GPS satellite system, obtained by removing from the measured

pseudo-range trend associated with changes in distance when satellite is moving.

It is seen that the presence of powerful stratocumulus clouds and rain zones increases RMS fluctuations of pseudo-range. Increasing the height of the clouds also affects the angles subtended by the greatest fluctuations of pseudo-range. Fig. 4 shows the variation of pseudo-range to the GPS system satellites in the propagation of the signal through the zone of continuous heavy rainfall.
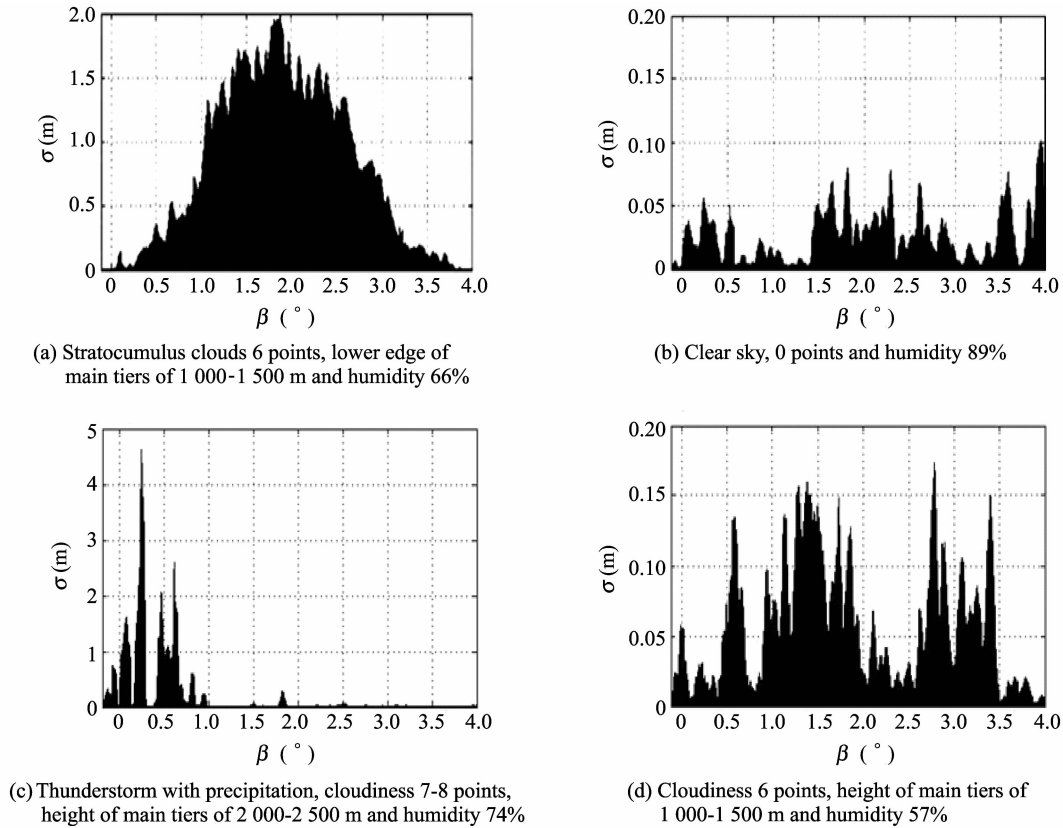
(a) Stratocumulus clouds 6 points, lower edge of
main tiers of 1 000-1 500 m and humidity 66%

(b) Clear sky, 0 points and humidity 89%

(c) Thunderstorm with precipitation, cloudiness 7-8 points,
height of main tiers of 2 000-2 500 m and humidity 74%

(d) Cloudiness 6 points, height of main tiers of
1 000-1 500 m and humidity 57%

Fig. 3   RMS value of pseudo-range fluctuations upon satellite's observation angle

(a) Variation of pseudorange to the satellites
for propagation through rainfall area

(b) Increment between adjacent pseudorange
measurements: 1 — During a rainstorm,
2 — In clear weather

(c) Pseudorange difference during
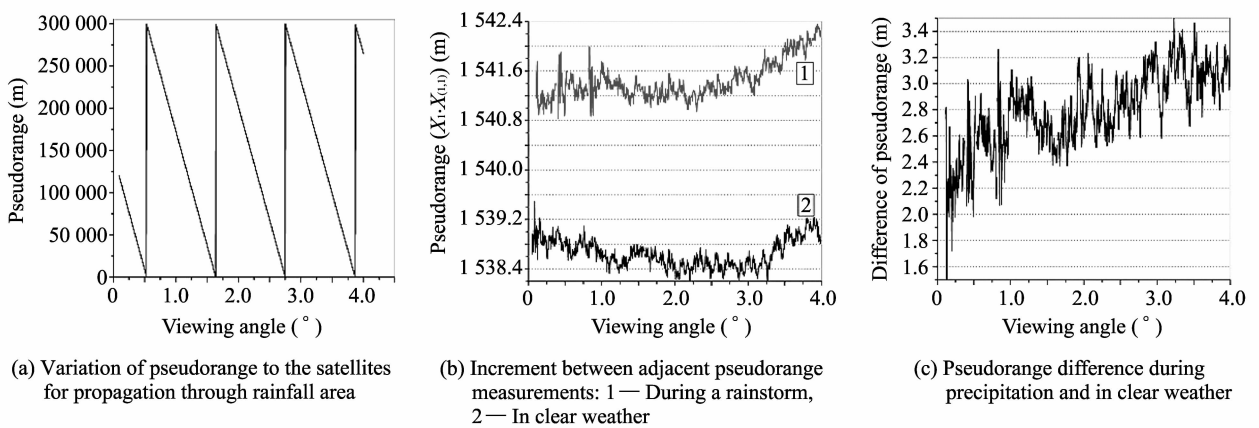precipitation and in clear weather

Fig. 4   Variation of pseudo-range to GPS system satellites in propagation of signal through zone of continuous heavy rainfall

It is obtained by removing from the measured pseudo-range trend (Fig. 4(a)) associated with the movement of the satellite and the resulting of change in slant range (Fig. 4(b)). The difference between the data with precipitation and without it is illustrated in Fig. 4.

Similarly, propagation through the zone of precipitation due to the increase of the measured pseudo-ranges decreases measured altitude Δz, as shown in Fig. 5. During precipitation, the measured altitude is

usually decreasing due to the increase of pseudo-ranges to satellites. Altitude measurement error due to propagation through the zone of precipitation may be masked by the diurnal variation of measurement error associated with the tropospheric refraction.

Fig. 6s(a) and (b) shows the daily altitude and surface refractive index value changes. It is seen that there is an increase in the measurement error in the evening and night hours，the nature of which repeats the changes in the surface refractive index value. These figures also show what happens when there was heavy rain. Comparison of altitudes measured during precipitation and in clear weather may allow the identification of changes due to delays in signal propagation through the zone of precipitation，as shown in Fig. 6.
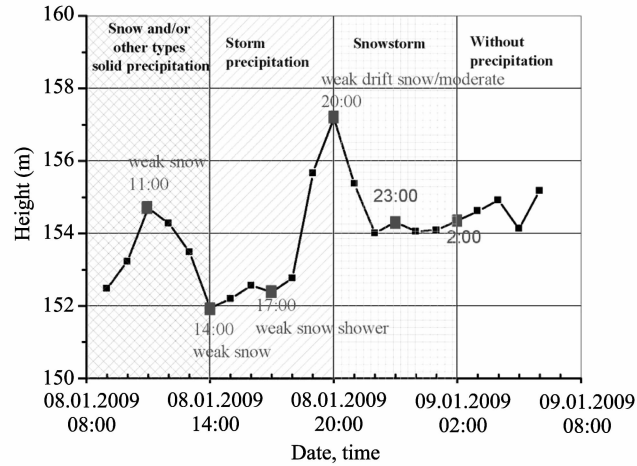

Fig. 5   Changes in measured altitude in propagation through zone of precipitation

(a) Altitude change for several days   (b) Changes in the surface refractive index value   (c) Altitude change due to rainfall
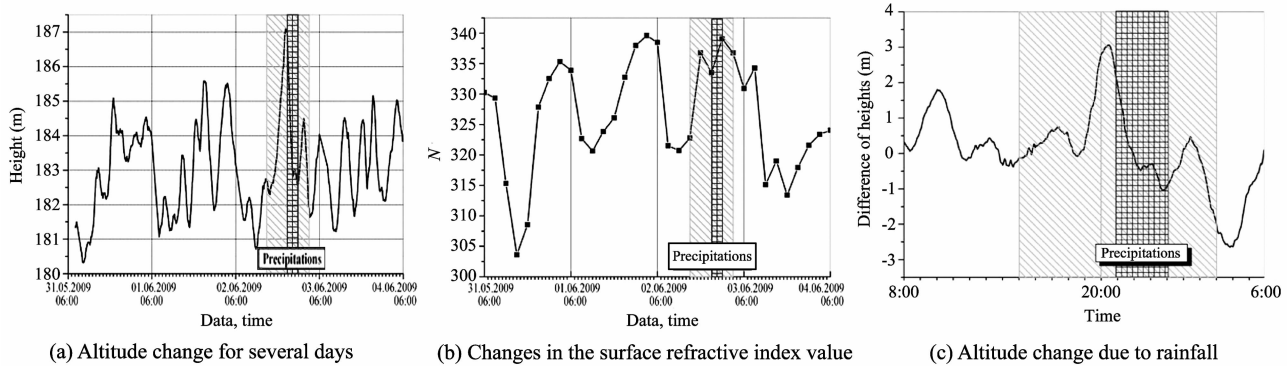
Fig. 6   Changing of the altitude and the refractive index of the troposphere

The altitudes obtained are compared by measuring the same satellite at the same time. Altitude measurement error associated with errors in determining pseudoranges Δr_i can be got by

$$\Delta z \approx \sum_{i=1}^{m} \Delta r_i \sin\psi\beta_i, \qquad (4)$$

where β_i is viewing angle for i-satellite，$m=4$ is their amount that is used in the measurements.

That at movement of satellites the troposphere inhomogeneities is moving in the areas is essential for propogation. This leads to an amplitude modulation of the received signal. The size n of the Fresnel zone at distances up to the satellite R_0 and inhomogeneities $l_0 = h_0/\sin\beta$, where h_0 its altitude，and β is the viewing angle of the satellite，taking into account that $R_0 \gg l_0$，is determined by the ratio[8]

$$r_n = \sqrt{n\frac{l_0(R_0-l_0)\lambda}{R_0}} \approx \sqrt{nl_0\lambda} = \sqrt{nh_0\lambda/\sin\beta}. \qquad (5)$$

The size of the Fresnel zones determines the spatial resolution of the inhomogeneities. It is for the height of the clouds for $1-4$ km is about $15-60$ m at $\beta =$

$90°$, increasing to $100-400$ m at elevation angles of about $1°$.

The angular size of the corresponding zone $\Delta\beta_n$ and the passage time Δr_n with its fixed point inhomogeneity due to the motion of the satellite in its orbit at a speed v_0 are defined by

$$\Delta\beta_n = \beta_n - \beta_{n-1} = \frac{r_n - r_{n-1}}{l_0},$$

$$\Delta t_n = \frac{\Delta\beta_n R_0}{v_0}. \qquad (6)$$

Completely,

$$\Delta\beta_n = \sqrt{n\frac{\lambda\sin\beta}{h_0}} - \sqrt{(n-1)\frac{\lambda\sin\beta}{h_0}},$$

$$\Delta t_m = \frac{\left(\sqrt{n\frac{\lambda\sin\beta}{h_0}} - \sqrt{(n-1)\frac{\lambda\sin\beta}{h_0}}\right)R_0}{v_0}. \qquad (7)$$

The first Fresnel zone equation takes the form

$$\Delta\beta_1 = \sqrt{\frac{\lambda\sin\beta}{h_0}},$$

$$\Delta t_1 = \frac{\left(\sqrt{\frac{\lambda\sin\beta}{h_0}}\right)R_0}{v_0}. \qquad (8)$$

Estimates with using Eq. (7) show that at the height of the troposphere inhomogeneities, such as outbreaks of thunderclouds $1-4$ km, the angular size of the first Fresnel zone for GPS satellites, located at the nadir, is about $1°-0.5°$. The movement time of the satellite at an angular size is $35-140$ s. At the same time, the small angle of sight satellites about $1°$ size of the area essential for propagation is a reduced to $0.1°$, and the time of its flight to $3.5-14$ s.

2   Conclusion

The possibility of detection of dangerous meteorological phenomena (areas of thunderstorm activity, saturated with water clouds) using the coordinate information receivers of satellite navigation systems is considered. The link between water content of clouds which shined through and the measured location, which can be used to identify areas of the hazardous meteorological phenomena is shown. It is experimentally shown that the presence of storm clouds and

precipitation leads to an increase in RMS value of the fluctuations of the measured pseudo-range. The calculated ratio that connect error of pseudo-range measurements with altitude, water content and viewing angles of the satellite are obtained. Based on the dielectric properties of water and water content of different types of clouds, it is estimated thet the expected change in pseudo-range depends on the intensity of rain. For heavy rainfall, they can amount to a few meters. The experimental results show that with the increase in intensity of the cloud cover, the appearance of zones of precipitation is manifested in an increase in the RMS value of the fluctuations of pseudo-range. Their value is in agreement with obtained theoretical estimates. To isolate the fluctuation component of pseudo-range, pseudo-differential method is used. In experimental studies, the receivers of navigation satellite system GPS, GLONASS CN-4701 and CN-4706 developed by Ltd. "NAVIS" have been used.

References

[1] Gudkov V N, Lutsenko V I, Lutsenko I V, et al. Detection of hazardous weather phenomena using receivers of global navigation satellite system. In: Proceedings of the 19th International Crimean Conference on Microwave & Telecommunication Technology, Sevastopol, 2009: 929-930.

[2] Hyatt H A. Emission, reflection and absorption of microwaves at a smooth air-water interface. Journal of Quantitative Spectroscopy Radiative Transfer, 1970, 10: 217-247.

[3] Kolosov M A, Armand N A, Yakovlev O I. Propagation at space communications. Communication, 1969: 155.

[4] Krassyuk N P, Koblov V L, Krassyuk V N. Effect of the troposphere and the underlying surface to RLS Work. Radio and Communication, 1988: 213.

[5] Kalinin A I. Propagation of radio waves on the tracks of terrestrial and space radio links. Communication, 1976: 296.

[6] Sukhonin E V. Attenuation of millimeter and submillimeter waves in the atmosphere with hydrometeors. Doctoral Dissertation of Phyical-Mathematic Sciences: 01. 04. 03 "Radiophysics", IRE Academy of Sciences USSR, Moscow, 1988.

[7] Royenko A N, Zamaraev B D, Kostin V L, et al. Scattering of millimeter radio waves with vegetation cover . In:

Proceedings of Radio Physics and Electronics，Kharkov，2002，7(2)：335-341.

［8］Dolukhanov propagation of radio waves. Communication，1965：400.

利用全球导航系统检测危险气象

V F Kravchenko[1] ，O V Kravchenko[1] ，V I Lutsenko[2] ，I V Lutsenko[2] ，D O Popov[2]

（1. Kotel'nikov Institute of Radio Engineering and Electronics，Russian Academy of Sciences，Moscow 125009，Russia；

2. Usikov Institute of Radiophysics and Electronics，National Academy of Sciences of Ukraine，Kharkov 61085，Ukraine)

摘　要： 提出了利用全球卫星导航系统和全球定位系统接收器得到的坐标测量数据进行危险气象现象检测的方法。依据伪距离和海拔高度的数据进行雷暴进程和强云团检测的可能性在理论上进行了演示，并在实验中加以确认。

关键词： 危险气象；无线辐射；全球导航系统；伪距；海拔高度